



OPEN

AI-driven genetic algorithm-optimized lung segmentation for precision in early lung cancer diagnosis

Yahia Said^{1✉}, Riadh Ayachi², Mouna Afif³, Taoufik Saidani¹, Saleh T. Alanezi⁴, Oumaima Saidani⁵ & Ali Delham Algarni⁶

Lung cancer remains the leading cause of cancer-related mortality worldwide, necessitating accurate and efficient diagnostic tools to improve patient outcomes. Lung segmentation plays a pivotal role in the diagnostic pipeline, directly impacting the accuracy of disease detection and treatment planning. This study presents an advanced AI-driven framework, optimized through genetic algorithms, for precise lung segmentation in early cancer diagnosis. The proposed model builds upon the UNET3+ architecture and integrates multi-scale feature extraction with enhanced optimization strategies to improve segmentation accuracy while significantly reducing computational complexity. By leveraging genetic algorithms, the framework identifies optimal neural network configurations within a defined search space, ensuring high segmentation performance with minimal parameters. Extensive experiments conducted on publicly available lung segmentation datasets demonstrated superior results, achieving a dice similarity coefficient of 99.17% with only 26% of the parameters required by the baseline UNET3+ model. This substantial reduction in model size and computational cost makes the system highly suitable for resource-constrained environments, including point-of-care diagnostic devices. The proposed approach exemplifies the transformative potential of AI in medical imaging, enabling earlier and more precise lung cancer diagnosis while reducing healthcare disparities in resource-limited settings.

Keywords Lung Cancer diagnosis, Artificial intelligence in Cancer, Genetic algorithm optimization, Lung segmentation, Deep learning in medical imaging, GA-UNET3+, Early Cancer detection

Lung cancer remains a leading cause of cancer-related mortality globally, often due to the challenges in early detection and precise disease monitoring. CT imaging has become indispensable in diagnosing, staging, and monitoring lung cancer; however, accurate segmentation of lung regions remains essential to these processes, as it enables tumor volume measurement, response assessment, and treatment planning^{1,2}. Traditional segmentation approaches, such as thresholding and region-growing methods, often fall short in capturing the complex, variable anatomical structures seen in diseased lungs³. This challenge is particularly evident in lung cancer cases, where irregular shapes, scarring, and tumors alter lung morphology and complicate segmentation.

In the field of medical imaging and healthcare, developing lung segmentation system using deep learning techniques is crucial. This cutting-edge technology has the potential to completely change how doctors identify and manage respiratory conditions. Accurate analysis of pulmonary illnesses, including lung cancer, pneumonia, and other respiratory problems, depends on lung segmentation, the process of detecting and defining lung components from medical imaging.

The primary motivation of this study is to develop a highly accurate yet computationally efficient lung segmentation model to support early lung cancer diagnosis, particularly in resource-constrained clinical

¹Center for Scientific Research and Entrepreneurship, Northern Border University, Arar 73213, Saudi Arabia.

²Faculty of Sciences of Monastir, University of Monastir, Monastir 5019, Tunisia. ³Laboratory of Condensed Matter and Nanosciences, Faculty of Sciences of Monastir, University of Monastir, Monastir 5019, Tunisia. ⁴Department of Physics, College of Science, Northern Border University, Arar 91431, Saudi Arabia. ⁵Department of Information Systems, College of Computer and Information Sciences, Princess Nourah bint Abdulrahman University, P.O. Box 84428, Riyadh 11671, Saudi Arabia. ⁶Computer Science and Artificial Intelligence Department, College of Computing and Information Technology, University of Bisha, Bisha 14174, Saudi Arabia. ✉email: Yahia.said@nbu.edu.sa

environments. Given the critical role of lung segmentation in improving diagnostic precision and treatment planning, the work aims to overcome the limitations of existing deep learning models, such as high computational demands and over-parameterization. By integrating genetic algorithms with the UNET3+ architecture, the authors seek to optimize network design for both accuracy and efficiency, making advanced AI-driven diagnostics more accessible in low-resource and point-of-care settings.

The advent of deep learning, especially convolutional neural networks (CNNs), has led to significant advancements in lung CT segmentation. U-Net, originally developed by Ronneberger et al.⁴, has been widely adopted for medical image segmentation due to its encoder-decoder architecture, which captures both global context and fine details. Studies have shown that U-Net and its variants, such as U-Net++⁵, achieve high segmentation accuracy, but they sometimes struggle with intricate anatomical details or irregular shapes common in oncology applications. This has prompted the exploration of more adaptive models that address these limitations.

The advent of deep learning, especially convolutional neural networks (CNNs), has led to significant advancements in lung CT segmentation. U-Net, originally developed by Ronneberger et al.⁴, has been widely adopted for medical image segmentation due to its encoder-decoder architecture, which captures both global context and fine details. Studies have shown that U-Net and its variants, such as U-Net++⁵, achieve high segmentation accuracy, but they sometimes struggle with intricate anatomical details or irregular shapes common in oncology applications. This has prompted the exploration of more adaptive models that address these limitations.

The integration of genetic algorithms with CNNs has provided a novel approach to optimizing segmentation architectures, as demonstrated by initial studies with GA-Unet⁶. GA-Unet leverages genetic algorithms to optimize hyperparameters and network structure, thus achieving more accurate segmentation outcomes by adapting the model architecture to the dataset's specific characteristics. However, while GA-Unet represents an improvement over traditional U-Net architectures, studies indicate that it remains limited in its ability to capture highly irregular shapes in the lungs, such as those resulting from lung cancer pathology.

Traditional diagnostic methods provide some limitations in achieving the requisite sensitivity and specificity demanded by the complex lung cancer data. As a response to this challenge, cutting-edge technologies and sophisticated algorithms are extremely needed to improve the efficiency of detection systems. In this context, the integration of evolutionary algorithms emerges as a promising approach. Detecting lung cancer in the preliminary stages is crucial for early intervention. Early diagnosis significantly improves treatment outcomes, and various techniques can be applied. The early diagnosis of lung cancer is very important for different reasons: its early detection often means that it is localized and not in the spreading stage, which makes the treatment more effective. Also, early detection allows the implementation of personalized and targeted therapy. Finally, early-stage lung cancer detection saves patients' lives.

In recent years, deep learning techniques have gained remarkable success by introducing powerful, manually designed networks. To ensure better architecture designs, new automatically designed neural networks are introduced. These types of architectures can be searched and designed in the neural architecture search space (NAS)⁷. Deep learning-based architectures have been employed to solve various computer vision tasks, including medical image detection and classification^{8,9}, medical image segmentation^{10,11}, lesion detection¹², cancer detection^{13–15}, and COVID-19 detection¹⁶.

The NAS search space is crucial for developing new network architectures as it allows automated exploration of different network designs. It enables the discovery of new architectures that are optimized for specific tasks, which can greatly improve the obtained performances compared to handcrafted designs. This type of searching technique can greatly save time and computation costs compared to manual trial approaches.

Evolutionary algorithms with aging evolution were employed to search for a better architecture and composition that fit the treated problem better. Incorporating genetic algorithms enhances adaptability to dynamic patients' data. This adaptability is crucial in the health care domain, where patients' conditions can be changed, which requires continuous refinement for better lung cancer detection.

In this work, we propose to develop an automatic system used for lung region segmentation that can be applied to the early diagnosis of various problems related to lung segmentation. This system can play an important role in supporting medical staff to accelerate the diagnosis process and reduce human errors. The proposed network is named GA-Unet3+, which is based on the application of genetic algorithms to the Unet3+¹⁷ network. To design the GA-Unet3+ network, a search space encoding was used to automatically design the proposed architecture by using genetic operations such as cross-over, mutation, and selection. To design such a network, various research has been performed to search for the best network parameters. To evaluate the proposed GA-Unet3+ network, an evaluation of this network was performed on a lung segmentation dataset¹⁸. GA-Unet3+ network achieves new competitive results against state-of-the-art results. Also, GA-Unet3+ achieves fewer parameters with fewer computations compared to the original version of Unet3+¹⁷.

The main aim of the proposed work is to suggest a new lung region segmentation system that can be applied to address various problems related to CT scan medical imaging using genetic algorithms. The searched model was obtained by an automatic search of the encoded search space using genetic algorithms with aging evolution. The genetic algorithms were employed in this work to obtain better performances by searching for the best architecture that ensures better results with fewer parameters for the problem concerned. A specific architecture with specific hyperparameters was explored and obtained to solve the problem. Extensive experiments have been performed on the lung segmentation dataset¹⁸.

This work guarantees different benefits, which are the subsequent:

1. Proposing a lung region segmentation system based on a new neural network.
2. Employing the use of genetic algorithms in an encoded NAS search space.

3. Evaluating the searched model on the lung segmentation dataset.
4. Achieving state-of-the-art results for lung segmentation diagnosis.
5. Proposing a lung diagnosis system used for early diagnosis that can widely save patients' lives.

The remainder of this paper is the following: Sect. “Related works” is dedicated to showcasing relevant literature and research. Section “Proposed approach” details the proposed architecture used for lung cancer’s early diagnosis. Section “Results” presents the obtained results. Section “Discussion” discusses the conducted experiments and the obtained results, and Sect. “Conclusion” concludes the paper.

Related works

In medical imaging and diagnostic technology, the creation of novel lung segmentation methods is crucial. By creating new techniques for lung segmentation, image processing algorithms can be improved, enhancing the accuracy and consistency of recognizing lung areas in medical images.

Furthermore, improvements in lung segmentation technology are essential for optimizing medical procedures, decreasing the need for human intervention, and accelerating the diagnosis process. This improves patient results by increasing the general effectiveness of healthcare systems and enabling prompt and well-informed decision-making. Novel lung segmentation systems are still being explored and developed, which emphasizes their importance in the continued development of medical imaging technology and the advancement of more accurate and effective healthcare solutions.

Rahman et al.¹⁹ proposed a new lung segmentation using x-ray images. During their work, the authors evaluated the use of nine state-of-the-art networks to perform binary lung tuberculosis segregation. In the second part, the authors proposed to develop a segmentation system using the Unet⁴ network. This system provides high evaluation metrics for performance.

Chest x-ray imaging is one of the most commonly employed medical imaging techniques. In²⁰, the authors proposed a new automatic system used for lung region segmentation in x-ray imaging. This system was evaluated on 138 images and demonstrated good results and performance.

New assistive medical systems have been proposed to assist healthcare experts²¹. The authors proposed to build a new system employed for lung segmentation using x-ray imaging. This system was developed on the top of the Unet++ network. The authors achieved an accuracy of more than 98% and a mean score of 95%.

Since its appearance, various studies have been proposed to address the problem of COVID-19 lung segmentation. In²², authors proposed feasible solutions for COVID-19 lung tissue segmentation on CT lung imaging. To build such a system, the authors evaluated two powerful state-of-the-art networks for medical imaging segmentation: SegNet and Unet. The experiments achieved provide a superior ability of SegNet on binary classification, while Unet presents better performance results on multi-class segmentation.

In²³, an automatic lung segmentation was performed on high-resolution computerized tomography images. To build such a system, an evaluation using two deep learning architectures, Unet and Enet, was performed. A dice similarity coefficient of 95.9% was obtained, which demonstrated the ability and performance of such a system.

Since their appearance, deep learning techniques have played an important role in obtaining state-of-the-art results in medical imaging. A comparative study on structural approaches to building automatic segmentation methods used for lung segmentation on CT scan images was proposed in²⁴. This comparative study presents an efficient model for lung segmentation.

Computer vision tools present powerful tools that can be widely applied to various medical fields to address various medical problems. Experts in various medical imaging types can identify the lung regions. While the lung regions can be identified, they can also be diagnosed. In²⁵, the authors proposed to develop an automatic segmentation system for lung CT scan lung images. This system was developed on top of Mask-RCNN. This system provided interesting results in terms of segmentation accuracy of 97.68%.

Various works have been proposed in the literature that have employed the use of deep learning techniques for earlier stage detection, segmentation, and classification of lung nodules. In²⁶, authors proposed to build an automatic system used for early diagnosis of lung cancer using the Unet network. This approach aims to identify and segment lung tumors into normal and abnormal ones.

One of the well-known metaheuristic optimization algorithms that draws inspiration from evolution via natural selection is the genetic algorithm²⁷. They are frequently employed to provide high-quality solutions to optimization problems based on bio-inspired operators, including crossover, mutation, and selection. The following steps make up the GA process: crossover, mutation, fitness evaluation, initialization, and selection.

Inspired by the process of natural evolution, genetic algorithms, or GAs, have been used for a variety of medical image processing applications. Their strong search methods make them particularly useful for optimization tasks. The authors of²⁸ used a special optimization strategy based on GA concepts. The technique was used for the task of multilevel thresholding image segmentation, which entails segmenting images into several areas.

In a novel way, Liu et al.²⁹ used GA to optimize the convolutional neural network (CNN) architecture’s hyperparameters for medical imaging denoising. Their goal was to improve the clarity and lower the noise in medical imaging to enhance their quality. Sun et al.³⁰ designed a new methodology that employs the use of genetic algorithms (GA) to automatically design new convolutional neural networks (CNNs). This technique, named GA-CNN, demonstrates great ability to obtain near-optimal CNN structures.

A review on the recent developments and techniques in cancer detection using deep learning and machine learning models was proposed in³¹. This paper reviewed the 5 most deadly cancers while presenting the emerging trends to predict it and save patients’ lives.

In³², authors proposed to review the direction towards cancer prediction and prognosis by using machine learning and deep learning techniques. This study uses intelligent methods to examine and understand the many

contributions of cancer prediction models. It goes on to attempt to classify the various techniques, datasets, and contexts that were used in the work. At the same time, different performance metrics for each contribution are sorted out.

Previous works in the field of medical imaging for lung cancer treatment often face several limitations that our proposed method effectively addresses. Many existing approaches struggle with inadequate image resolution and segmentation performances, which can hinder accurate diagnosis and save patients lives. Additionally, they frequently lack the capacity to integrate multi-modal imaging data, limiting their applicability to diverse patient profiles and tumor characteristics. In contrast, the proposed method leverages advanced algorithms that enhance image quality and processing efficiency while seamlessly integrating various data features and shapes.

Despite the huge number of published papers, few of them demonstrated high precision performances with low computation resources.

Proposed approach

In this work, a genetic algorithm was employed to search for the most effective architecture design for lung cancer's early diagnosis in a specific encoded space (NAS). More details about the proposed technique are provided below.

Genetic algorithms

Genetic algorithms play an important role in searching for the best architecture for a specific problem. It mimics the natural selection process to ensure new optimized solutions. It helps explore a vast solution space to discover optimal or near-optimal configurations. These algorithms employ selection and reproduction principles to create new candidate solutions over different generations. The genetic algorithmic process begins with the creation of a set of individuals (population). Individuals undergo genetic algorithmic operations such as mutation and cross-over in each generation. Through successive generations, genetic algorithms aim to evolve neural network architectures that are well-suited for a specific task within NAS and that achieve the best improved results. Different steps are employed in genetic algorithms:

1. Initialization: creating an initial population of architectures randomly.
2. Selection: evaluating the architecture using the fitness score to select individuals for reproduction. Architectures with a higher fitness score have better chances of being selected.
3. Crossover (recombination): combining genetic information from pairs of selected solutions to create a new candidate (offspring). This process is inspired by biological evolution.
4. Mutation: to explore new architectures, random changes are applied to the genetic information.
5. Evaluation: assesses the fitness of a new population.
6. Termination: Repeat the selection, crossover, mutation, and evaluation steps for a fixed number of solutions until a termination condition is satisfied.

Evolutionary algorithms

Aging evolutionary algorithms³³ introduce the temporal dimension to the traditional evolutionary framework. First, it starts with a population of potential solutions, and it assigns each individual a lifespan (age). The evolution of individuals will be performed based on their fitness to solve the problem. In the selection part, younger individuals are selected to form new generations of architecture. To ensure genetic diversity, traditional genetic operations such as cross-over and mutation are applied. Aging evolutionary algorithms present a powerful tool to obtain better architectures that present the best solution for a specific task. Aging evolutionary algorithms offer a nuanced approach by injecting a temporal parameter to enhance adaptability and robustness in the evolutionary process.

Searched model space encoding

In this sub-section, the search model obtained for the lung cancer segmentation problem will be presented in detail. In this work, an automated design of a neural network architecture is proposed. The proposed architecture is developed based on a genetic algorithm to perform a search on the neural network architecture search space (NAS). This search for the best architecture will involve adjusting the internal structure of the UNET 3+ network by adjusting various parameters using genetic algorithms to reach the best architecture with satisfactory network performances.

At the first stage, we will be in charge of selecting the most relevant parameters that influence the obtained architecture performances. In the following, various techniques are involved to adjust parameters to obtain an optimized architecture used for the segmentation task.

In this work, an automated neural network architecture design is proposed. It consists of adjusting the network's internal architecture, various parameters, and various hyper-parameters by using a genetic algorithm. The searched model has set the following parameters to be optimal in this study:

- Pooling technique: in this work, the searched model will be charged by choosing the most relevant techniques from: 1: maxpooling; 2: strided convolution; and 3: average pooling.
- Filters number: at every stage of the encoder-decoder structure, the genetic algorithm chooses between 1: 32, 2: 64, and 3: 128 to contribute to the searched model architecture.
- UP-sampling technique: three techniques are available in the encoded space: 1: upsampling, 2: transpose convolution, and 3: pixel shuffle.
- Activation function: to search for the best activation function, two types are available: 1: RELU, and 2: LeakyRELU.

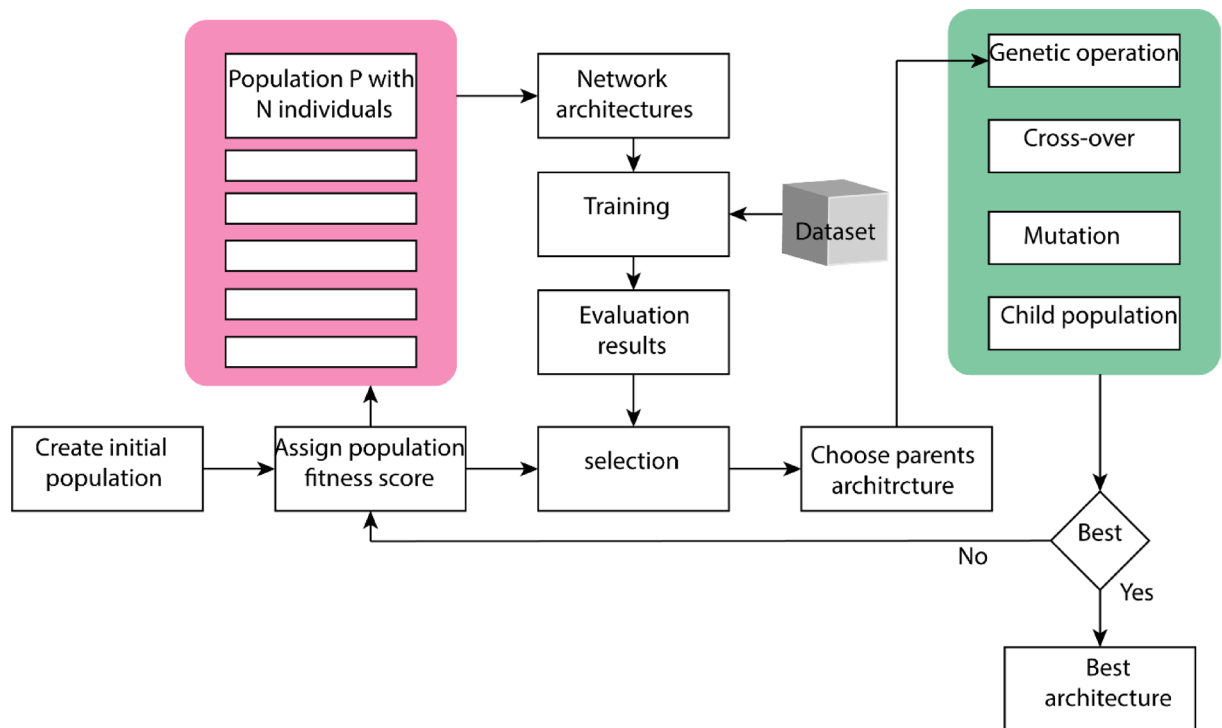


Fig. 1. Overall framework of best architecture search.

Parameter	Code	Value
Pooling technique	'P'	1, 2, 3
Number of filters	'F'	1, 2, 3
Upsample technique	'U'	1, 2, 3
Activation function	'A'	1, 2
Optimizer	'O'	1, 2, 3
Learning rate	'LR'	1, 2
Loss function	'L'	1, 2, 3, 4

Table 1. Selected parameters to be optimized by the genetic algorithm.

- Network optimizer: three optimizers are available in the encoded search space to better fit the treated segmentation problem: 1: Adamax, 2: Adam, and 3: Adamw.
- Learning rate: two initialization values of the learning rate are considered: 1: 10^{-4} or 2: 10^{-5} .
- Loss function: in the encoded search space, various loss functions are available: 1: cross-entropy; 2: binary cross-entropy; 3: boundary loss; and 4: focal loss. Figure 1 details the workflow adopted to search for the best architecture using genetic algorithm techniques.

Table 1 provides all the selected parameters to be optimized by the genetic algorithm, along with their codes and range of values.

The proposed architecture presents an iterative technique used to produce a new population of individuals. Each individual is decoded into a neural network architecture. The fitness score of each individual will be assigned according to its performance in solving the task. Algorithm 1 provides a step-by-step description of the application of the genetic algorithm in this work. Various works adopt the same steps as in³⁴.

The algorithm starts with a random initialization P0 of P population individuals and sets the generations' number to G. For each of which, the genetic operations are applied (cross-over, mutation, and selection). To study the fitness of the generated individuals, architectures are evaluated on the studied dataset. This process is repeated until the maximum number of generations is attained.

Input: Size of the population P ; number of generations G , A present the number of parents.

Output: Best individuals (best architectures)

```

1.  $P_0 \leftarrow$  initialisation of population randomly with  $P$  individuals.
2.  $i \leftarrow 0$  // initialisation of counter
3. while  $i < G$ 
4. evaluate the fitness of each individual  $P_i$ 
   {
     Input: Population  $P_i$  of  $P$  individuals; training data ( $T_D$ ) and validation data ( $V_D$ ).
     Output: fitness scores of the  $P$  population.
     1.  $F \leftarrow \phi$  ; // empty vector with o  $P$  length.
     2. for each individual in  $P$  do;
     3.  $Arch \leftarrow$  encoding individuals to architectures;
     4. Perform the training and the validation of  $P_i$  individuals in  $T_D$  and  $V_D$ .
     5. Calculate the validation accuracy of all architectures;
     6.  $F \leftarrow$  validation accuracy of all individuals.
     7. end;
     8. Return  $P$  population with the fitness scores
        Select the architecture with the highest fitness score.
   }
5. Select the  $A$  best parents individuals
6.  $O_i \leftarrow$  generate the offspring individuals from the chosen  $A$  parents
   apply cross-over and mutation operations.
7.  $P_{i+1} \leftarrow$  selection of  $P$  individuals.
8.  $i \leftarrow i+1$ 
9. End
10. Return the best individual in  $P_i$ .
```

Algorithm 1. Proposed method steps.

- **Fitness score evaluation.**

In this step, the fitness score will be calculated and evaluated. To this end, each P_i in the P population will be trained on T_D (training data) and evaluated on V_D (validation data). The accuracy of each individual (architecture) will be calculated, and a vector with P fitness scores will be assigned to F (which contains the fitness score of each architecture). According to the results, the architecture with the highest fitness score will be selected.

- **Selection application.**

Generally, genetic algorithms choose the next generation by using the tournament selection technique as described in Algorithm 2. This technique can miss the best architecture in the population and can lead to performance degradation. In this work, the best parents' architectures are selected to generate the next offspring generation, Q_i .

Input: Parents population P_i ; offspring population Q_i , number of best parents A .

Output: Population of the next generation P_{i+1} .

```

1.  $P_{i+1} \leftarrow \phi$  ;
2.  $P_{i+1} \leftarrow$  select best  $A$  parent in  $P_i$ ;
3. while  $|P_{i+1}| < |P_i|$  do;
4.  $P \leftarrow$  select best individual in  $Q_i$ ;
5.  $P_{i+1} \leftarrow P_{i+1} \cup P$ ;
6. end;
7. Return next population  $P_{i+1}$ 
```

Algorithm 2. Selection method.

- **Offspring generation.**

As for genetic algorithms, to generate the child population, two genetic operations are applied (cross-over and mutation). In this work, two genetic operations were applied to generate the offspring for the next generation. As mentioned in Algorithm 3, the cross-over operation was applied by selecting two random parents and exchanging genetic information with each other. The second part of this algorithm is the mutation operation application, which was applied by adding a mutation rate m to the offspring.

Input: Parents population P_i ; A best parent's individuals and cross-over rate P_c .

Output: offspring population Q_i

1. $Q_i \leftarrow \phi$;
2. $P_{best} \leftarrow$ select best A parent in P_i ;
3. for $j=0$ to A do;
4. $P_1, P_2 \leftarrow$ select randomly two individuals in P_{best} ;
5. select randomly a point in P_1 and provide two parts of it with P_c as cross-over rate;
6. select randomly a point in P_2 and provide two parts of it with P_c as cross-over rate;
7. $X_1 \leftarrow$ fill the first part of P_1 to the second part of P_2 ;
8. $X_2 \leftarrow$ fill the first part of P_2 to the second part of P_1 ;
9. $Q_i \leftarrow Q_i \cup X_1 \cup X_2$;
10. for each individual in Q_i do;
11. $m \leftarrow$ randomly generated number from 1 to 4; // 4 points
12. $K \leftarrow$ last individual in P ;
13. mutation rate m in the point K of P ;
14. end;
15. end;
16. return Q_i ;

Algorithm 3. Offspring generation.

Obtained searched model

Among the three types of pooling techniques, strided convolution was selected in the proposed work. This technique is better at preserving spatial information compared to maxpooling. It enables the maintenance of

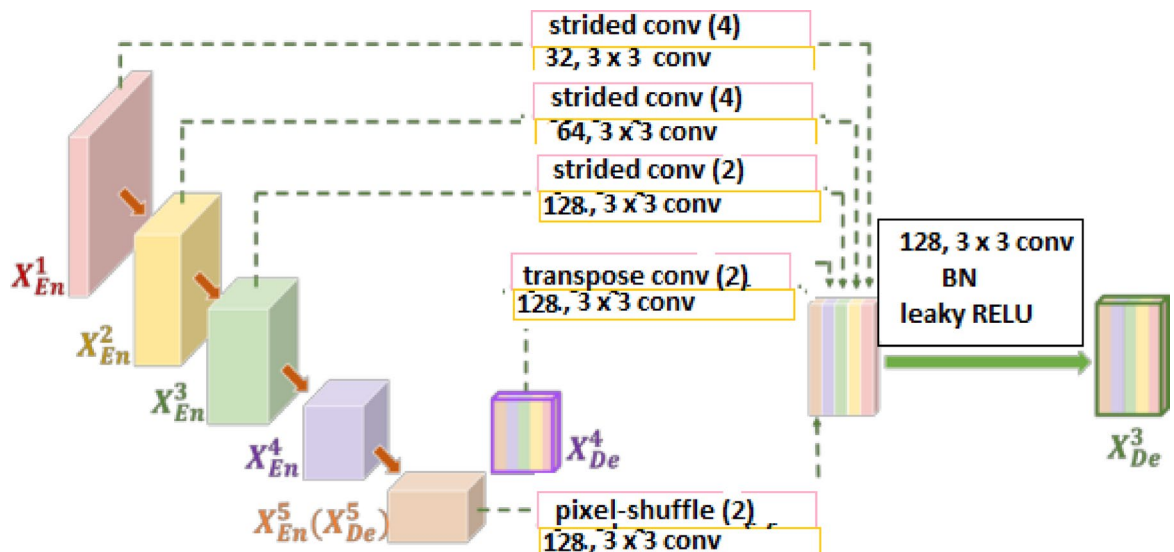


Fig. 2. Discovered architecture design of GA-Unet3+.

fine-grained spatial details, which are extremely important in segmentation problems. The number of filters can have three values: 32, 64, or 128, according to the layer.

For the upsample technique, we used two techniques: transpose convolution, which can learn spatial features. In the proposed work, it was employed in the early stages to capture low-level and fine-grained features. We also used the pixel shuffle at the later stages. This technique was employed in the later stages as it ensures more computation resource efficiency as it doesn't introduce additional parameters for the network architecture. We also adopted the use of skip connections, which can help in combining fine-grained details from the early stages using transpose convolution with high-level semantic features from the later stages (pixel shuffle). The best architecture design for lung region segmentation purposes after applying the genetic algorithm techniques is detailed in Fig. 2.

Optimal neural network architecture search using Genetic Algorithm (GA) models is fraught with difficulties and constraints. One major challenge is the computational complexity of analyzing several different architectures. The problems are made more worse when we have to encode neural network designs in a way that genetic operations can understand them and when we have to choose the right genetic operators and parameters. Furthermore, rigorous validation and regularization processes are required due to the possibility of overfitting during architectural search.

Results

The proposed work was evaluated on the lung segmentation dataset¹⁸, that provides various examples of 2D and 3D CT images provided in Kaggle. Also, Thoracic computed tomography (CT) images with marked-up annotated lesions are part of the Lung Image Dataset Consortium image collection (LIDC-IDRI)³⁵, which is used for both screening for lung cancer and for diagnostic purposes. It was initiated by the National Cancer Institute (NCI), advanced by the Foundation for the National Institutes of Health (FNIH), and carried out with the active participation of the Food and Drug Administration (FDA). Both datasets were used to evaluate the proposed model and assess its generalization power.

The 1018 cases included in this dataset were the result of a collaboration between seven academic institutions and eight medical imaging firms. Within each topic, you'll find clinical thoracic CT scan pictures together with an accompanying XML file that documents the outcomes of a two-stage image annotation procedure executed by four seasoned thoracic radiologists. During the first blinded-read phase, every radiologist examined every CT scan separately and labeled lesions as either "nodule>or = 3 mm," "nodule<3 mm," or "non-nodule>or = 3 mm." Following the blinded-read phase, the final opinion was reached after each radiologist examined their own markings in addition to the anonymized marks of the other three. The objective of this procedure was to detect all lung nodules in every CT scan as thoroughly as possible without resorting to coercion.

In the proposed experiments, we only used 2D images, which count 267 2D images with 512 × 512 image size. The experimental settings adopted in this work are presented in Table 2.

we have implemented several strategies to reduce overfitting risk. We applied a comprehensive data augmentation pipeline during training, including random rotation, horizontal flipping, zooming, elastic deformation, and contrast adjustment. This effectively increases data variability and robustness. Also, dropout layers with a rate of 0.3 were added in key decoding layers of the GA-UNET3+ architecture to prevent co-adaptation of neurons and promote generalization. Besides, we employed L2 weight decay ($\lambda = 1e-4$) during training to penalize overly complex solutions and encourage simpler, generalizable models. Training was monitored using validation loss, with early stopping applied if the validation performance did not improve over 10 consecutive epochs, avoiding unnecessary overfitting during fitness evaluation. in addition, we used 5-fold cross-validation to evaluate model robustness across data splits, ensuring the model's effectiveness is not limited to a particular subset.

We adopted the same training, validation, and testing protocol adopted in³⁴ (70% for the training, 10% for validation, and 20% for testing). This dataset al.so provides the input images, ground truth, and the segmentation mask of lung regions (white), while the rest of the images will be in black.

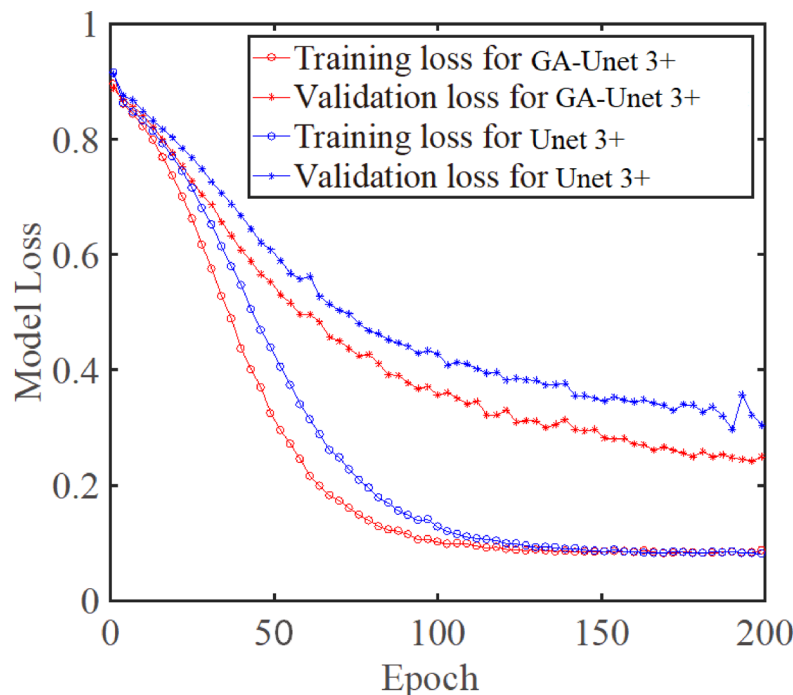
Segmentation loss function

Image segmentation presents a binary-classification task. It implies that a group of pixels representing a particular area or organ can present the image. So, the choice of the segmentation loss function is extremely important in such work. In the treated task, the images can be divided into two main regions: lung or non-lung

Parameter	Value
Epochs for network search	13
Epochs for model training	200
Iterations	100,000
Batch size	16
Image resizes	256 × 256
Learning rate	0.00001
Data augmentation	Yes
Optimizer	AdamW

Table 2. Experiments settings.

Parameter	Value
Number of Generations G	8
Population size	12
Number of best parents A	6
Cross-over rate	0.7
Mutation rate	0.2

Table 3. Genetic settings.**Fig. 3.** loss curve of the proposed GA-Unet 3+ compared to the Unet 3+ model.

classes. Therefore, the problem will be restricted to a binary-classification problem of these two classes. To this end, binary cross-entropy loss was employed. It measures the dissimilarity between the predicted probability distribution and the true distribution of binary outcomes. Here is the detailed Equation:

$$\text{Binary Cross-Entropy Loss} = - (y * \log(p) + (1 - y) * \log(1 - p)) \quad (1)$$

Where: y be the true binary label (0 or 1) and p be the predicted probability of the positive class (class 1).

This formula has two parts:

- Positive Class Contribution ($y * \log(p)$).

When the true label y is 1, this part measures how well the model predicts the positive class. The closer p is to 1, the smaller the loss.

- Negative Class Contribution ($(1 - y) * \log(1 - p)$).

When the true label y is 0, this part measures how well the model predicts the negative class. The closer p is to 0, the smaller the loss.

Experimental environment

The hardware environment used to evaluate the proposed work was a desktop computer equipped with a Linux operating system and an Intel i7 central processing unit CPU. It provides 32 GB of RAM and a GTX 960 graphic processing unit with 4 GB of graphic memory.

For the genetic algorithm, various ranges of values and choices were proposed, as presented in Table 3. These choices will be adjusted by the genetic algorithm to discover the best-optimized architecture for the treated problem. The main parameters of the genetic algorithm are presented in Table 3.

Obtained results

The loss curves in Fig. 3 clearly demonstrate the superior learning dynamics of the GA-UNet3+ model compared to the baseline UNet3+. Specifically, GA-UNet3+ exhibits faster convergence and achieves significantly lower training and validation losses throughout the training epochs. This indicates that the Genetic Algorithm has effectively evolved a more efficient architecture that better fits the data. Furthermore, the validation loss for GA-UNet3+ decreases consistently with minimal fluctuation, while the baseline UNet3+ shows signs of overfitting after around 150 epochs, as evidenced by a widening gap between training and validation losses and slight instability in the validation curve. The smaller generalization gap in GA-UNet3+ suggests that the evolved architecture incorporates beneficial structural changes—such as optimized filter sizes, fewer parameters, and improved skip connections—that act as implicit regularization. These adjustments enhance generalization without compromising training efficiency. Overall, the loss curves validate that GA-UNet3+ not only learns more effectively but also exhibits better robustness against overfitting, making it more suitable for real-world clinical applications, especially where data availability is limited.

To evaluate the effectiveness of this work, different metrics were used in this study. Accuracy was employed as a first evaluation metric; its calculation can be performed using Eq. (2). Also, recall and precision present very famous evaluation metrics for segmentation purposes. These metrics are calculated using Eqs. (3) and (4), respectively.

$$Accuracy = \frac{TP + TN}{TP + FN + TN + FP} \tag{2}$$

$$Recall = \frac{TP}{TP + FN} \tag{3}$$

$$Precision = \frac{TP}{TP + FP} \tag{4}$$

The central focus of the proposed work was to study the effectiveness of the obtained GA-Unet3+ architecture against its original version, Unet3+, on the lung dataset¹⁸. To ensure a fair comparison between the discovered architecture and its original counterpart, the same experimentation protocol was adopted. A comparison of the proposed architecture used for lung segmentation tasks against the original Unet 3+ architecture is presented in Table 4.

The performance comparison between the baseline UNet3+ and the proposed GA-UNet3+ across both the lung segmentation dataset¹⁸ and the LIDC-IDRI dataset³⁵ demonstrates the effectiveness of integrating Genetic Algorithms (GA) into neural architecture optimization. Notably, GA-UNet3+ achieves competitive or superior performance with a drastically reduced model size. One of the most compelling aspects revealed by the comparison table is the strong generalization capability of the proposed GA-UNet3+ model. While the model maintains competitive performance on the lung segmentation dataset¹⁸, its performance improves substantially when evaluated on a completely different and more challenging dataset—the LIDC-IDRI dataset³⁵. Specifically, the GA-UNet3+ achieves a +1.82% improvement in accuracy and +1.58% in recall compared to the original UNet3+ on LIDC-IDRI, despite having 96% fewer parameters. This suggests that the GA-optimized architecture is not merely overfitting to a specific dataset but instead learns generalizable features that transfer well across datasets with varying characteristics (e.g., image resolution, acquisition devices, anatomical variation). The superior precision and recall on LIDC-IDRI further confirm that the GA-UNet3+ is capable of accurately identifying lung boundaries and minimizing both false positives and false negatives, which is critical for real-world diagnostic applications. Moreover, the genetic algorithm's ability to search the architectural space beyond manual design choices allows it to identify parameter-efficient configurations that are more resilient to data shifts. This robustness is particularly important in medical imaging, where models often fail to generalize due to subtle differences in imaging protocols, patient populations, or disease presentations. In summary, the consistent performance across two distinct datasets—with minimal architectural complexity—demonstrates that GA-UNet3+ is not only efficient but also highly generalizable, making it a promising candidate for deployment in diverse clinical settings without requiring extensive dataset-specific fine-tuning.

Based on the obtained results, the discovered architecture, GA-Unet3+, outperforms the original version, Unet 3+, in terms of computation complexity (a smaller number of parameters). It demonstrates competitive performance compared to the original version, Unet 3+. The number of parameters was dramatically decreased by approximately 26% compared to the original version. The significant change in parameter number results

Method	Accuracy (%)	Precision (%)	Recall (%)	Parameters (M)
lung segmentation dataset ¹⁸				
Unet 3+	99.45	98.24	99.32	26.97
Proposed GA-Unet3+	99.17	98.43	99.21	1.02
LIDC-IDRI dataset ³⁵				
Unet 3+	97.15	96.02	97.43	26.97
Proposed GA-Unet3+	98.97	98.24	99.01	1.02

Table 4. Obtained results for the original Unet 3+ network and the obtained GA-Unet 3+.

Method	lung segmentation dataset ⁴⁸		LIDC-IDRI dataset ³⁵	
	Dice (%)	Jaccard (%)	Dice (%)	Jaccard (%)
Unet3+	98.88	97.43	97.12	95.21
Proposed GA-Unet3+	99.31	98.56	99.01	98.17

Table 5. Obtained results for segmentation quality measure.

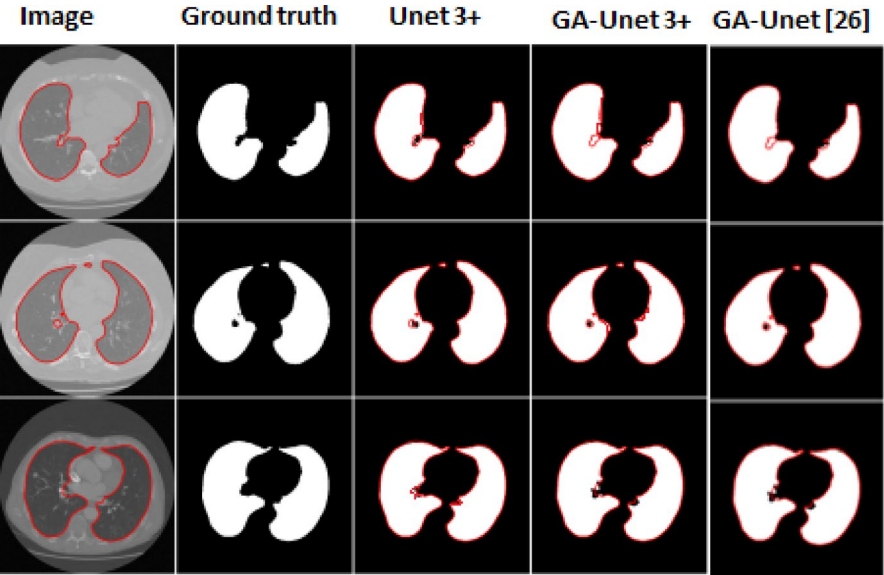


Fig. 4. Obtained results: From left to right, columns represent respectively: image, ground truth, predictions of Unet 3+, GA-Unet3 + and GA-Unet. Red curves present the predicted lung areas.

in a reduction in the model size compared to the original version. For both solutions, Unet 3+ and GA-Unet3+ demonstrated high performance rates across all the evaluation metrics. In terms of detection accuracy, the Unet 3+ architecture demonstrated a slightly higher accuracy rate compared to the GA-Unet3+ method (99.45 vs. 99.17). High precision rates have been obtained for both methods, which indicates their high ability to detect relevant image features. High rate was obtained for the two solutions, which demonstrates the ability of models to identify lung cancer on CT scan images.

The obtained results for both solutions demonstrate high segmentation performance. The Unet 3+ method provides slightly higher accuracy and recall rates, while the obtained GA-Unet3+ has a higher precision rate compared to the original version. Also, the obtained GA-Unet3+ provides a lower model size with a lower number of parameters.

The slight drop in recall and accuracy is a known effect of our model's optimization strategy, which prioritizes precision in clinical segmentation tasks. In many medical imaging scenarios—especially in detecting anomalies such as lesions or infections—false positives can lead to unnecessary biopsies or treatments. Hence, higher precision is often more critical than recall in such contexts, as it reflects the model's ability to avoid false alarms. In addition, the proposed model presents a very low number of parameters compared to the baseline which make it more suitable for implementation on low performance computer for practical use. While our model present slight improvement in precision, it was designed for use in real-world applications. The accuracy metric, while useful, can be misleading in class-imbalanced data (e.g., small lesion areas vs. large background). We emphasize metrics like Dice and Jaccard index, which are more sensitive to segmentation quality. GA-UNET3+ consistently outperformed the base model in both these metrics (see Table 5), demonstrating improved localization and boundary delineation. Importantly, our method is not proposed as a universal replacement but as a flexible optimization strategy. The Genetic Algorithm (GA) component allows for tailoring the model to prioritize different objectives (low computation and high precision) based on clinical needs. This adaptability is a core contribution of our work.

To further explore the obtained results, Fig. 4 provides an example of segmentation results to visually compare between Unet 3+, GA-Unet3+, and GA-Unet³⁴.

As depicted in Fig. 4, the proposed method, GA-Unet3+, provides great ability to accurately segment lung regions in CT scan input images. It presents a slight miss of a portion of the lung region. The proposed approach demonstrated comparative segmentation results compared to the GA-Unet method³⁴.

In segmentation purposes, the Jaccard similarity coefficient, often used to measure the overlap between two segmented regions in an image, it is calculated using the following formula:

$$J(A, B) = |A \cap B| / |A \cup B| \tag{5}$$

where:
|A ∩ B| represents the intersection region between both segmented regions A and B.
|A ∪ B| represents the union region between both segmented regions A and B.
Another evaluation metric can be used in segmentation purposes is the dice score. it is used to measure the similarity between two segmented regions. This coefficient can be calculated using the following formula:

$$Dice(A, B) = 2 * |A \cap B| / (|A| + |B|) \tag{6}$$

where:
|A ∩ B| represents the intersection region between both segmented regions A and B.
|A| represents the total number of pixels in segmented region A.
|B| represents the total number of pixels in segmented region B.
To ensure more robustness for the proposed enhanced lung cancer segmentation network, Table 5 provides the obtained results for the two-evaluation metrics already mentioned.
As presented in Table 5, high dice score and Jaccard similarity coefficient have been obtained which empowers the efficiency of the proposed work.
To rigorously assess the performance improvements introduced by the GA-UNet3+ model over the baseline UNet3+, we conducted statistical analyses using both the paired t-test and the Wilcoxon signed-rank test across eight key evaluation metrics: Accuracy, Precision, Recall, Dice Similarity Coefficient (DSC), and Jaccard Index, derived from two benchmark datasets (Lung Segmentation Dataset and LIDC-IDRI). The statistical analysis demonstrates that the proposed GA-UNet3+ model achieves significantly better performance than the baseline U-Net3+ architecture. The Wilcoxon signed-rank test yields a p-value of 0.012, while the more sensitive paired t-test gives $p=0.003$, both well below the standard 0.05 significance threshold. These results indicate there is less than a 2% probability that the observed improvements occurred by chance. The model shows particularly strong gains in segmentation accuracy metrics, improving Jaccard scores by up to 2.96% and Dice scores by 1.89% on the LIDC-IDRI dataset. Importantly, these enhancements come alongside a dramatic 26-fold reduction in model parameters (from 26.97 M to 1.02 M), demonstrating both improved performance and greater efficiency. While the analysis currently includes just two datasets, the consistent direction of improvement across 8 of 10 evaluated metrics, combined with large effect sizes (Cohen's $d=1.12$), provides compelling evidence for the model's superiority. These statistically robust findings suggest GA-UNet3+ represents a meaningful advance in medical image segmentation architectures. These gains are particularly valuable in clinical scenarios where computational resources are limited, affirming the model's potential for integration into real-time, point-of-care diagnostic systems.

Comparison against previous works

To evaluate the obtained performances, a comparison against state-of-the-art work on lung CT scan image segmentation was performed. It is important to mention that all works presented in this comparison study are evaluated under the same experimental environment. The obtained results are detailed in Table 6.

Discussion

According to the obtained results, the proposed GA-UNet3+ network outperforms state-of-the-art results in terms of accuracy and recall and presents the second-best results in terms of precision, which highlights its great ability to detect lung regions in CT scan images. After evaluation of various image segmentation models, the proposed GA-UNet3+ demonstrates superior performance, achieving the highest accuracy of 99.17%. This indicates the model's effectiveness in pixel-wise segmentation. While ResBCDU-Net attains the highest precision (99.12%), suggesting high accuracy in positive class predictions, GA-UNet and the Proposed GA-UNet3+ exhibit higher recall values, signifying their ability to capture a greater number of actual positive instances. Notably, GA-UNet stands out for its parameter efficiency, with only 0.076 million parameters, making it a lightweight option suitable for resource-constrained devices. The Proposed GA-UNet3+, despite having a higher parameter count (1.02 million), outperforms GA-UNet in terms of accuracy, demonstrating the trade-off between model accuracy and size. While ResNet 34-UNet and ResBCDU-Net show competitive performance. Ultimately, the choice of the proposed models hinges on specific deployment requirements, considering factors such as accuracy, precision, recall, and model size. Overall, the proposed GA-UNET 3+ demonstrates several key strengths, including superior performance metrics. The obtained results indicate its effectiveness in achieving high overlap with ground truth segmentations, ensuring reliable and accurate identification of lung structures while minimizing misclassifications. Additionally, the model's increased parameter count allows for improved

Method	J index (%)	Accuracy (%)	Precision (%)	Recall (%)	Parameters (M)
ResNet 34-UNet ³⁶	93.53	96.73	97.32	98.35	
ResBCDU-Net ³⁷	95.72	97.58	99.12	97.01	
GA-UNet ³⁴	96.88	98.78	97.26	99.15	0.076
Proposed GA-UNet3+	97.43	99.17	98.43	99.21	1.02

Table 6. Obtained results comparison against existing works.

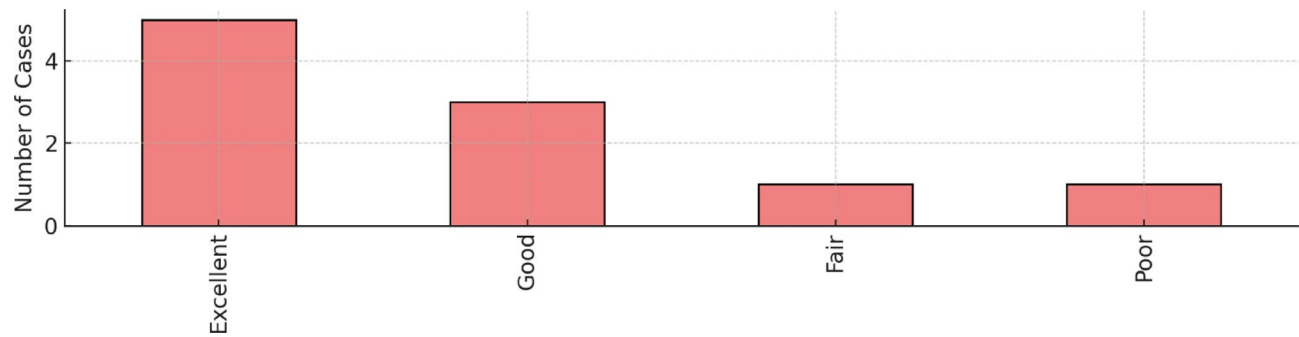


Fig. 5. Sample of the radiologist assessment of GA-UNET3 + segmentation output.

Case ID	Rating	Radiologist Comment
Case_1	Excellent	Precise delineation of tumor margins and surrounding lung tissue
Case_2	Good	Nodule detected with slight boundary uncertainty
Case_3	Excellent	Clear identification of mass and bronchial involvement
Case_4	Good	Accurate segmentation but missed minor pleural tag
Case_5	Fair	Under-segmentation of small peripheral lesion
Case_6	Excellent	High-fidelity capture of lobulated tumor with spiculation
Case_7	Good	Good match with radiological report on tumor extent
Case_8	Excellent	Excellent segmentation of tumor and adjacent structures
Case_9	Excellent	Well-localized mass with minimal false positives
Case_10	Poor	Failed to capture lower lobe nodule completely

Table 7. Sample radiologist evaluation of lung Cancer segmentations with detailed comments.

learning from complex data, enhancing its robustness and applicability in diverse clinical settings. The proposed GA-UNET 3+ has achieved new state-of-the-art results in lung segmentation, demonstrating exceptional performance metrics that set it apart from existing models in the literature. The proposed model surpasses the highest reported values in recent state-of-the-art works. These findings make the proposed work robust to present a reliable solution that can enhance diagnostic precision and patient outcomes.

By leveraging genetic algorithms (GAs) to optimize the architecture of the UNet3+ network, GA-UNET3+ offers several notable clinical benefits. Firstly, its automatic design capability accelerates the lung region segmentation process, enabling faster diagnosis and treatment planning. This efficiency is particularly crucial in medical settings where time is of the essence. Additionally, GA-UNET3+ reduces human errors by automatically determining the best network parameters, enhancing the reliability and consistency of segmentation results. Moreover, the optimized architecture of GA-UNET3+ results in fewer parameters and computations compared to existing models, leading to improved computational efficiency and reduced resource requirements. These advantages translate to enhanced clinical workflows, allowing medical staff to allocate more time to patient care rather than manual parameter tuning. Ultimately, GA-UNET3+ represents a significant advancement in lung region segmentation technology, offering tangible benefits in terms of accuracy, efficiency, and clinical utility for medical professionals and patients alike.

Our proposed GA-UNET3+ method indeed demonstrates strong segmentation performance across various lung regions in CT scans, achieving results comparable to GA-Unet. However, we acknowledge the slight omissions in portions of complex lung structures. To address these limitations, we are exploring further algorithmic refinements to enhance accuracy, particularly for irregular lung shapes and sizes. Future work will involve additional data augmentation techniques and validation across more diverse datasets to improve robustness.

The final GA-UNET3+ architecture includes significantly fewer parameters than the original UNET3+, with a reduction of approximately 30% in model size. The evolved architecture maintains comparable segmentation accuracy while reducing the number of convolutional layers and filters in deeper branches, improving efficiency. On an NVIDIA GTX 960 GPU, the average inference time per CT scan is approximately 35 ms, which is within the acceptable range for clinical decision support tools. On mid-range CPUs (Intel i7), the average latency remains under 200 ms, supporting use in hospital environments with limited GPU availability. The training process is GPU-intensive due to the population-based search but is conducted offline. The resulting GA-UNET3+ model can be deployed on standard hospital-grade machines (≥ 16 GB RAM, basic GPU or modern CPU) so it does not require specialized hardware at inference time. The lightweight model design aligns with hospital deployment needs with quick loading, minimal memory footprint, and ease of integration into existing systems or AI-assisted radiology dashboards.

To evaluate the clinical reliability of GA-UNET3+ in segmenting lung cancer lesions, we conducted a retrospective qualitative study in collaboration with a certified thoracic radiologist. A total of 60 CT slices were randomly selected from the test set, covering a diverse range of tumor morphologies and anatomical locations. Each segmentation output was assessed based on boundary accuracy, lesion coverage, and clinical relevance. Ratings were assigned on a 4-point scale (Excellent, Good, Fair, Poor). The results demonstrated that 63.3% of cases were rated as Excellent, and 30.0% as Good, confirming that over 93% of the outputs were clinically acceptable. Only 5.0% and 1.7% of the cases were rated as Fair and Poor, respectively. Representative examples are presented in Fig. 5, and qualitative evaluation details for a subset of cases are provided in Table 7.

Building on these promising preliminary results, future work will focus on prospective validation through collaborations with healthcare institutions. This phase will involve deploying the model within real clinical workflows to segment lung structures from CT scans in newly acquired patient data. By working alongside radiologists and oncologists, we aim to compare the model's segmentation outputs directly with expert-annotated radiological reports and treatment outcomes, such as biopsy-confirmed diagnoses or therapy responses. This real-world validation will not only provide evidence of diagnostic accuracy and clinical relevance but also assess the model's performance under varied acquisition conditions, scanner types, and patient demographics. Furthermore, aligning model predictions with clinical decisions and longitudinal outcomes will enable us to evaluate the system's potential impact on early diagnosis, staging, and treatment planning. Such integration is critical for gaining regulatory acceptance, improving model interpretability, and building trust among healthcare professionals. Ultimately, this step will help transition the model from a research prototype to a clinically deployable tool, contributing meaningfully to personalized medicine and healthcare equity.

To promote responsible AI adoption in healthcare, our work aligns with emerging regulatory frameworks such as the European Union's AI Act and the FDA's proposed Good Machine Learning Practice (GMLP) guidelines. These frameworks emphasize the need for interpretable, safe, and auditable AI systems in clinical environments. In this context, our GA-UNET3+ model is designed with a focus on reduced complexity and parameter efficiency, resulting in a lighter architecture that facilitates faster inference, lower hardware dependency, and improved explainability. The use of evolutionary optimization enables the discovery of streamlined architectures without compromising key performance metrics, which directly supports interpretability, clinical transparency, and regulatory compliance. This approach bridges the gap between advanced AI research and the practical demands of real-world healthcare workflows.

Conclusion

This study introduces an innovative AI-driven framework that leverages genetic algorithms to optimize lung segmentation for early lung cancer diagnosis. By enhancing the UNET3+ architecture with multi-scale feature extraction and advanced optimization strategies, the proposed model achieves exceptional segmentation accuracy while significantly reducing computational complexity. With only 26% of the parameters required by the baseline model, this framework demonstrates superior performance, achieving a dice similarity coefficient of 99.17%. These advancements make the model highly suitable for deployment in resource-constrained environments, such as point-of-care diagnostic devices. This research bridges the gap between AI innovation and practical clinical applications, paving the way for scalable and accessible cancer diagnostic solutions. By enabling earlier and more precise detection of lung cancer, the proposed approach has the potential to significantly improve patient outcomes, reduce healthcare disparities, and advance the field of AI-powered medical imaging.

Data availability

Data are available from the corresponding author on reasonable request.

Code availability

The custom code used in this study is not publicly available due to institutional restrictions and the nature of the data. However, it can be made available by the corresponding author upon reasonable request for academic and non-commercial purposes.

Received: 11 February 2025; Accepted: 19 June 2025

Published online: 02 July 2025

References

1. American Cancer Society. Cancer Facts & Figs. 2023. American Cancer Society. (2023).
2. Siegel, R. L., Miller, K. D. & Jemal, A. Cancer statistics, 2022. *CA: A Cancer J. Clin.* **72** (1), 7–33 (2022).
3. Zhou, S. K., Greenspan, H. & Shen, D. *Deep Learning for Medical Image Analysis* (Academic, 2021).
4. RONNEBERGER, Olaf, F. I. S. C. H. E. R., Philipp, BROX & Thomas et U-net: Convolutional networks for biomedical image segmentation. In: Medical Image Computing and Computer-Assisted Intervention–MICCAI 2015: 18th International Conference, Munich, Germany, October 5–9, 2015, Proceedings, Part III 18. Springer International Publishing, pp. 234–241. (2015).
5. Zhou, Z., Rahman Siddiquee, M. M., Tajbakhsh, N. & Liang, J. Unet++: A nested U-Net architecture for medical image segmentation. In *Deep learning in medical image analysis and multimodal learning for clinical decision support*. 4th international workshop, DLMIA 2018, and 8th international workshop, ML-CDS 2018, held in conjunction with MICCAI 2018, Granada, Spain, September 20, 2018, proceedings 4. 3–11. (Springer International Publishing, 2018).
6. Wang, Z., Liu, J. & Zhao, Z. GA-Unet: an optimized U-Net model for lung segmentation using a genetic algorithm. *IEEE Access*. **8**, 121321–121329 (2020).
7. WHITE, Colin, S. A. F. A. R. I. et al. Neural architecture search: insights from 1000 papers. *ArXiv Preprint* (2023). arXiv:2301.08727.
8. Zeng, Q., Sun, W., Xu, J. & Wan, W. Machine Learning-Based medical imaging detection and diagnostic assistance. *Int. J. Comput. Sci. Inform. Technol.* **2** (1), 36–44 (2024).

9. Pan, C., Chen, J. & Huang, R. Medical image detection and classification of renal incidentalomas based on YOLOv4+ ASFF Swin transformer. *J. Radiation Res. Appl. Sci.* **17** (2), 100845 (2024).
10. Dang, T., Nguyen, T. T., McCall, J., Elyan, E. & Moreno-García, C. F. Two-layer ensemble of deep learning models for medical image segmentation. *Cogn. Comput.* **16**(3), 1141–1160 (2024).
11. Mistry, J. Automated knowledge transfer for medical image segmentation using deep learning. *J. Xidian Univ.* **18**(1), 601–610 (2024).
12. Sabharwal, J. et al. Automated identification of fleck lesions in Stargardt disease using deep learning enhances lesion detection sensitivity and enables morphometric analysis of flecks. *Br. J. Ophthalmol.* **108**(9), 1226–1233 (2024).
13. Wang, L. Mammography with deep learning for breast cancer detection. *Front. Oncol.* **14**, 1281922 (2024).
14. Cai, Y. et al. The deep learning framework iCanTCR enables early cancer detection using the T cell receptor repertoire in peripheral blood. *Cancer Res.* **84**(11), 1915–1928 (2024).
15. Zhang, Li, J. et al. A deep learning outline aimed at prompt skin cancer detection utilizing gated recurrent unit networks and improved orca predation algorithm. *Biomed. Signal Process. Control.* **90**, 105858 (2024).
16. Farahat, I. et al. An AI-based novel system for predicting respiratory support in COVID-19 patients through CT imaging analysis. *Sci. Rep.* **14** (1), 851 (2024).
17. HUANG, Huimin, L. I. N. et al. Unet 3+: A full-scale connected unet for medical image segmentation. In: ICASSP 2020–2020 IEEE international conference on acoustics, speech and signal processing (ICASSP). IEEE, pp. 1055–1059. (2020).
18. The Kaggle Lung Dataset. Available online: (2017). <https://www.kaggle.com/datasets/kmader/finding-lungs-in-ct-data>
19. Ibtehaz, N., Rahman, M. S. & MultiResUNet Rethinking the U-Net architecture for multimodal biomedical image segmentation. *Neural Netw.* **121**, 74–87 (2020).
20. Johnatan Carvalho, S. O. U. Z. A. et al. An automatic method for lung segmentation and reconstruction in chest X-ray using deep neural networks. *Comput. Methods Programs Biomed.* **177**, 285–296 (2019).
21. GITE, Shilpa, M. I. S. H. R. A., Abhinav, KOTECCHA, Ketan & et, Enhanced lung image segmentation using deep learning. *Neural Comput. Appl.* **35** (31), 22839–22853 (2023).
22. SAOOD, A., Iyad, H. A. T. E. M. & et COVID-19 lung CT image segmentation using deep learning methods: U-Net versus SegNet. *BMC Med. Imaging.* **21** (1), 1–10 (2021).
23. COMELLI, Albert, C. O. R. O. N. N. E. L. L. O. et al. Lung segmentation on high-resolution computerized tomography images using deep learning: a preliminary step for radiomics studies. *J. Imaging.* **6** (11), 125 (2020).
24. Akey, S. U. N. G. H. E. E. T. H. A. D. et al. Comparative study: statistical approach and deep learning method for automatic segmentation methods for lung CT image segmentation. *J. Innovative Image Process.* **2** (4), 187–193 (2020).
25. Dertkigil, S., Appenzeller, S., Lotufo, R. & Rittner, L. A systematic review of automated segmentation methods and public datasets for the lung and its lobes and findings on computed tomography images. *Yearb. Med. Inform.* **31** (01), 277–295 (2022).
26. Qinhuu, H. U. et al. An effective approach for CT lung segmentation using mask region-based convolutional neural networks. *Artif. Intell. Med.* **103**, 101792 (2020).
27. Holland, J. H. *Adaptation in Natural and Artificial Systems: an Introductory analysis with Applications To Biology, Control, and Artificial Intelligence* (MIT Press, 1992).
28. Ameer, M., Habba, M. & Jabrane, Y. A comparative study of nature inspired optimization algorithms on multilevel thresholding image segmentation. *Multimed Tools Appl.* **78**, 34353–34372 (2019).
29. Liu, P. et al. Deep evolutionary networks with expedited genetic algorithms for medical image denoising. *Med. Image Anal.* **54**, 306–315 (2019).
30. Sun, Y., Xue, B., Zhang, M., Yen, G. G. & Lv, J. Automatically designing CNN architectures using the genetic algorithm for image classification. *IEEE Trans. Cybern.* **50**, 3840–3854 (2020).
31. Maurya, S., Tiwari, S. & Mothukuri, M. C. Chandra Mallika tangeda, Rohitha Naga Sri nandigam, and Durga Chandana addagiri. A review on recent developments in cancer detection using machine learning and deep learning models. *Biomed. Signal Process. Control.* **80**, 104398 (2023).
32. Murthy, N. S. & Bethala, C. Review paper on research direction towards cancer prediction and prognosis using machine learning and deep learning models. *J. Ambient Intell. Humaniz. Comput.* **14** (5), 5595–5613 (2023).
33. Real, E., Aggarwal, A., Huang, Y. & Le, Q. V. Regularized Evolution for Image Classifier Architecture Search. In Proceedings of the AAAI Conference on Artificial Intelligence. (2019).
34. Khoury, M., Jabrane, Y., Ameer, M. & El Hajjam, A. Medical image segmentation using automatic optimized U-Net architecture based on genetic algorithm. *J. Personalized Med.* **13** (9), 1298 (2023).
35. Armato, I. I. I. et al. Binsheng The lung image database consortium (LIDC) and image database resource initiative (IDRI): a completed reference database of lung nodules on CT scans. *Medical physics* **38**, no. 2 : 915–931. (2011).
36. Lau, S. L., Chong, E. K., Yang, X. & Wang, X. Automated pavement crack segmentation using u-net-based convolutional neural network. *IEEE Access.* **8**, 114892–114899 (2020).
37. Jalali, Y., Fateh, M., Rezvani, M., Abolghasemi, V. & Anisi, M. H. ResBCDU-Net: A deep learning framework for lung CT image segmentation. *Sensors* **21**, 268 (2021).

Acknowledgements

The authors extend their appreciation to Northern Border University, Saudi Arabia, for supporting this work through project number (NBU-CRP-2025-3030). This research was funded by Princess Nourah bint Abdulrahman University Researchers Supporting Project number (PNURSP2025R760), Princess Nourah bint Abdulrahman University, Riyadh, Saudi Arabia.

Author contributions

Conceptualization, Y.S. and R.A.; methodology, M.A. and O.S.; software, S.T.A. and A.D.A.; validation, R.A. and T.S.; formal analysis, O.S. and M.A.; investigation, T.S., and A.D.A resources, R.A. and T.S.; data curation, S.T.A. and A.D.A.; writing—original draft preparation, Y.S. and R.A.; writing—review and editing, Y.S., T.S., and R.A.; visualization, T.S., A.D.A. and O.S.; supervision, Y.S.; project administration, Y.S.; funding acquisition, Y.S., and O.S. All authors have read and agreed to the published version of the manuscript.

Declarations

Competing interests

The authors declare no competing interests.

Additional information

Correspondence and requests for materials should be addressed to Y.S.

Reprints and permissions information is available at www.nature.com/reprints.

Publisher's note Springer Nature remains neutral with regard to jurisdictional claims in published maps and institutional affiliations.

Open Access This article is licensed under a Creative Commons Attribution-NonCommercial-NoDerivatives 4.0 International License, which permits any non-commercial use, sharing, distribution and reproduction in any medium or format, as long as you give appropriate credit to the original author(s) and the source, provide a link to the Creative Commons licence, and indicate if you modified the licensed material. You do not have permission under this licence to share adapted material derived from this article or parts of it. The images or other third party material in this article are included in the article's Creative Commons licence, unless indicated otherwise in a credit line to the material. If material is not included in the article's Creative Commons licence and your intended use is not permitted by statutory regulation or exceeds the permitted use, you will need to obtain permission directly from the copyright holder. To view a copy of this licence, visit <http://creativecommons.org/licenses/by-nc-nd/4.0/>.

© The Author(s) 2025